

Semantic Example Guided Image-to-Image Translation

Jialu Huang, Jing Liao, Tak Wu Sam Kwong
 Department of Computer Science
 City University of Hong Kong

Abstract—Many image-to-image (I2I) translation problems are in nature of high diversity that a single input may have various counterparts. Prior works proposed the multi-modal network that can build a many-to-many mapping between two visual domains. However, most of them are guided by sampled noises. Some others encode the reference images into a latent vector, by which the semantic information of the reference image will be washed away. In this work, we aim to provide a solution to control the output based on references semantically. Given a reference image and an input in another domain, a semantic matching is first performed between the two visual contents and generates the auxiliary image, which is explicitly encouraged to preserve semantic characteristics of the reference. A deep network then is used for I2I translation and the final outputs are expected to be semantically similar to both the input and the reference; however, no such paired data can satisfy that dual-similarity in a supervised fashion, so we build up a self-supervised framework to serve the training purpose. We improve the quality and diversity of the outputs by employing non-local blocks and a multi-task architecture. We assess the proposed method through extensive qualitative and quantitative evaluations and also presented comparisons with several state-of-art models.

I. INTRODUCTION

Image-to-image(I2I) translation by deep neural networks shed lights on many vision and graphics applications, such as image synthesis(sketch/label/artwork to photos), colorization(grayscale to color), image enhancement(low-resolution to high resolution), etc. Deep neural networks that can learn a mapping between two visual domains and generate images in the target domain with a certain level of diversity could become a set of powerful tools in industrial design, digital art and animation/game production.

The pioneering work Pix2pix[11] designed a single-modal network as a general-purpose solution to the I2I problems, which is then followed by the CycleGAN[37] claiming that, with cycle consistency, unpaired data can also be used as raw materials to cook an outstanding I2I model. However, the I2I problem is in nature of high diversity that it is possible for one image in the source domain to have multiple counterparts in the target domain. Therefore researchers proposed multi-modal networks that can generate various images corresponding to one input. Recent progress shows that lots of the multi-modal network are driven by noise vectors that different noise inputs may finally generate different images. Since noise vectors cannot provide specific guidance, a large number of experiments are then required to achieve desired results. Besides, modal collapse can frequently occur to this type of network due to that generator may ignore the additional noise in training[19], [13].

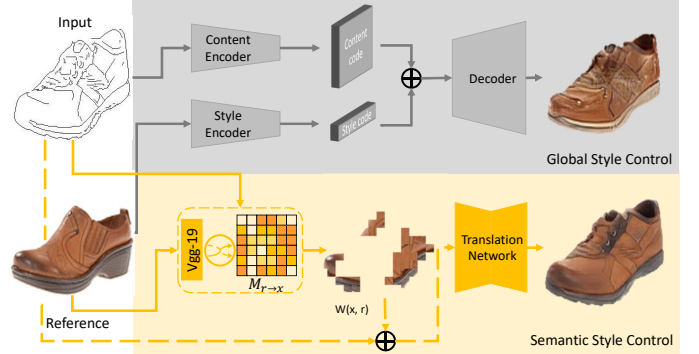


Fig. 1: Comparison between conventional global style control and our proposed semantic example based style control. The global style control can only generate images with overall similarities to the reference but our semantic style control preserve the characteristic of the reference with semantic matching. It can be observed that color, the styles of shoe sole and leather material can be preserved in this example while the shoe generated by conventional method can only inherit general color of the reference. The correspondence map $M_{r \rightarrow x}$ and the auxiliary image $W(x, r)$ will be introduced with details in the section III.

Some multi-modal network guided by images or attributes were then proposed [13], [10], inspired by Gatys' Style transfer[6], a common approach is to learn a low-dimensional style latent code of the reference image and then use it to reconstruct the output image, we name it as "Global Style Control" shown in Fig.1. This method can generate results similar to the reference at an overall level but cannot guarantee semantic similarity with details. To our knowledge, existing methods cannot perform semantically local control automatically in the I2I translation.

An ideal solution is to train a model that can not only learn a mapping between two visual domains but also absorb semantically related information from the reference images. This problem can be described in a more general way as a semantic exemplar-based multi-modal I2I problem, given two sets of images in different domains $\mathcal{X} \subset \mathbb{R}^{H \times W \times C}$, $\mathcal{Y} \subset \mathbb{R}^{H \times W \times C}$ and a set of reference images $r \in \mathcal{Y}$, we train a model $G : (\mathcal{X}|r) \rightarrow \mathcal{Y}^r$. The output $\hat{y} = G(x|r)$ should be domain-wise indistinguishable from images $y \in \mathcal{Y}$ and contains semantic affinity to the image $r \in \mathcal{Y}$. Here $\mathcal{Y}^r \subset \mathcal{Y}$ refers to a sub-domain of \mathcal{Y} that contains images of similar appearance style to r . This problem is, however, challenging for two main

reasons: (1) lack of grouped data (x, r, \hat{y}) , the output \hat{y} should be in the target domain and contain visual attributes of the reference r , this kind of data is scarce and difficult to obtain. (2) Semantic incompatibility that the correspondence is first established between the input and the reference, since they may not have the same semantic attributes, mismatches can happen during this process. Therefore, the quality of the result depends heavily on the choice of reference.

In this work, we present a self-supervised network that uses parts of reference images with semantic affinity to the input image as guidance to ensure their semantic consistency. Compared to the aforementioned models with local control, our network only requires a reference image, which is of high flexibility and hence makes batch production possible in applications and manufactures.

To achieve these goals, first, we design a pre-processing module that can build up a semantic mapping between the input and the reference, generating a warped image as auxiliary data with visual attributes of the reference and preserving the structure of the input image. We explore the self-supervised method by constructing training data to conquer the difficulty that lack of grouped data. With paired data $\{x, y\}$ where $x \in \mathcal{X}, y \in \mathcal{Y}$, we warp y to x and obtain a warped image y' . Then we use y' as the reference for the input x in the training stage. However, y' may have much more similarities with x compared to the random reference used in real tests. Hence we intentionally manipulate the warped images by shifting and adding noise, which aims to simulate mismatches and inconsistencies in color, shape, locations that G will encounter in the test process. We then design a multi-task architecture and non-local blocks to ameliorate performance in terms of feature selection and guidance propagation.

Compared with conventional global style control mentioned in [10], [23], latent style code are extracted by an encoder in the form of a vector, after combining with the content structure, the final output can inherit overall style from the reference, shown in Fig.1(top part). However, this cannot achieve semantic control within a specific small region, since spatial information is lost if the style code is stored in a vector. We propose the semantic-match process to provide utmost semantic guidance for each sub-region. With the self-supervised method, reliable guidance will be preserved since they contribute little to the reconstruction loss while the unreliable guidance will be discarded and modified.

We show that our model can be applied in various datasets and achieve reasonable results transferred to the target domain with local semantic similarities to the reference images. We assessed the proposed method through extensive qualitative and quantitative evaluations, and our model presents competitive performance against the state-of-art methods. Additionally, a detailed ablation study in terms of both network architectures and losses functions demonstrate the effectiveness of our proposed model for multi-model I2I problem.

Our major contributions are listed as follows:

- We propose the first semantic example guided I2I translation solution, which can not only transfer images from one domain to another with style control based on the

reference but also guarantee the output images to have semantic similarities with the reference.

- To solve the problem that the lack of grouped data, we designed a data configuration procedure, which then allows us to perform the translation in a self-supervised fashion.
- We build up a new I2I model including a semantic-matching block and a translation network. Non-local layers and multi-task architecture are adopted to achieve higher image quality

II. RELATED WORK

Single-modal I2I translation Recent attempts for I2I translation built on the pix2pix[11] model, which uses a conditional generative adversarial model to learn a mapping between two visual domains. It is then followed by CycleGAN[37] that proposes cycle consistency as the core component of their objective, which provides adequate constraint to support training with unpaired data. Related work [16] proposed by Liu et al. assumes that images in different domains can be mapped to a shared latent space with the same latent code.

Multi-modal I2I translation However, those frameworks are single-modal networks that can only output one image at a time, which is of low efficiency compared with training time. To tackle this problem, several research works [5], [7], [3] proposed methods that can generate a discrete number of outputs with the same input. Later, Zhu et al. proposed BicycleGAN[38], which can achieve many-to-many I2I translation with unlimited outputs. MUNIT[10] proposed by Huang et al. is also an outstanding multi-modal framework trained with unpaired data. Also, inspired by CycleGAN[37], Almahairi et al. proposed the Augmented CycleGAN[1] which can learn many-to-many mappings by cycling over the original domains augmented with auxiliary latent spaces.

I2I translation with global control A significant limitation of most of these work is that generated outputs cannot be controlled explicitly. It was briefly mentioned in MUNIT[10] that style code could be extracted from the reference image and recombine it with the content code of the input image to generate an image containing similar style as the reference. Instead of extracting latent style code, Lee et al.[13] disentangles the latent spaces of x and y into a shared content space and an attribute space respectively, and reconstruct the image by applying a cross-cycle consistency loss. Related works[18], [8] also tried to manipulate latent space and encourage the model to generate multiple outputs based on provided references. However, separating and modifying the latent space can only ensure the similarity at an overall level, it cannot partially control the output image with such reference.

I2I translation with local control Few works focus on the local control in I2I translation, most of them require extract assistance from users, Zhang et al. [35] propose a locally controlled coloration method required color indication from users at different locations. You et al.[31] proposed a method to transfer the image from edge domain with sparse color input. However, this method required carefully prepared guidance which provides detailed color distribution and position alignment with the input sketch.

non-GAN based methods In addition, there are also non-GAN based image synthesis works. Deep Image Analysis (DIA) proposed by Liao et al.[14] is a representative work of iteration based traditional image synthesis method, by computing a match map between features from an image pair, it can generate an output preserving the content structure of one image as well as style attributes from the other. Bansal et al. proposed PixelNN (PNN) a simple nearest-neighbor (NN) approach that synthesizes high-frequency photo-realistic images from an "incomplete" signal[4], aims to solve the modal collapse issue introduced by GAN. PNN proposed another match method that using nearest-neighbor search method to learn the mapping between images and generates images preserving styles from different references. However, those methods may generate incorrect or invalid results once the corresponding map is inaccurate. Our proposed method shows robustness handling corresponding matching with noise, detailed comparison and discussion are shown in the following sections.

III. SEMANTIC EXAMPLE GUIDED I2I TRANSLATION NETWORK (SEGIN)

Our proposed I2I model G consists of two parts, a preprocess module S to match the x and the r semantically, which is then followed by the translation network N for I2I translation. Given an input image $x \in \mathcal{X}$ and a reference image $r \in \mathcal{Y}$, we first match image patches between x and r and generate an auxiliary image $\mathcal{W}(x, r)$, which contains superficial details of the reference and also maintains the basic structure of the input image. Both x and r are then fed into N with auxiliary image \mathcal{W} , where the input image will be transferred to the target domain and meanwhile preserving the semantic similarities to the reference image. We provide an instantiation of the model $G : (\mathcal{X}|r) \rightarrow \mathcal{Y}^r$ that the input image x , the final output \hat{y} and reference r contain a set of sub-regions $\{x_1, x_2, \dots, x_n\}$, $\{\hat{y}_1, \hat{y}_2, \dots, \hat{y}_n\}$ and $\{r_1, r_2, \dots, r_n\}$ respectively, then $\exists i, j \in \{1, 2, \dots, n\}$ that $\hat{y}_i \sim x_i$ and $\hat{y}_i \sim r_j$ if the input image features around the sub-region i is semantically related to that of the sub-region j in the reference r , where " $A \sim B$ " indicates that A is similar to B in pixel-wise. The architecture of our model Semantic Example Guided I2I translation Network (SEGIN) is shown in Fig.2 and details will be presented and discussed as follows.

A. Semantic Match

As shown in Fig.3, image features of the input and the reference are first extracted by a pre-trained VGG-19 [27]. Those features are then unfolded by the vectorization operation, followed by generation of corresponding map $M_{r \rightarrow x}$ between image features from different sources. We then construct the auxiliary image by adopting image patches from the reference according to indication provided by the corresponding map. Spatially and semantically similar patches such as regions marked by the blue boxes on the reference shoes can still be kept, which will then pass to the final outputs.

Define $\kappa(\cdot)$ as a vectorization operation that transforms a matrix into a vector with row priority and let $\kappa(\Phi(x))$ denotes a vector of all the image feature patches of x with length

of n , where the image features $\Phi(x)$ are extracted by VGG-19[27]. Our goal is to match the features between the reference and the input image. For each patch $\kappa(\Phi(x))_i$ with size of $k \times k \times C$, where C is the number of channels, we find its most similar feature patch $\kappa(\Phi(r))_j$ in the reference by minimizing its cosine distance and build up a similarity map ξ :

$$\xi_i = \arg \max_{j=1,2,\dots,n} \frac{\kappa(\Phi(x))_i \cdot \kappa(\Phi(r))_j}{|\kappa(\Phi(x))_i| \cdot |\kappa(\Phi(r))_j|} \quad (1)$$

Different from other image reconstruction methods mentioned in previous work [13], [33], [10] such that combines a compressed latent style code with the content, which is then sent to the decoder and obtain the output. Semantic and spatial information may be washed away during this process [23]. We first construct the auxiliary image by adopting image patches in r directly. Let $\kappa(r)$ represents a list of image patches extracted from r with the same length as $\kappa(\Phi(r))$. The size of image patches $\kappa(r)$ is $\delta k \times \delta k \times 3$ where δ is the scaling parameter and $\delta = size(r)/size(\Phi(r))$. Then, we define the reconstructed image as $\mathcal{W}(x, r)$ that

$$\kappa(\mathcal{W}(x, r))_i := \kappa(r)_{\xi_i} \quad (2)$$

With a transform from vector to matrix $\kappa^{-1}(\cdot)$, we can obtain the auxiliary image $\mathcal{W}(x, r)$ that not only contains the superficial details of the reference image with semantic similarities but also conserves the major structure of the input image. In this stage, we try to provide utmost semantically similar patches stored in $\mathcal{W}(x, r)$ as initial guidance for the local control.

B. Translation Network

1) **Data construction for Self-supervised model:** According to the problem definition, the final output should belong to the target domain and preserve the semantically similar regions of r . This process requires a conditioned mapping $G : (\mathcal{X}|r) \rightarrow \mathcal{Y}^r$, which is different from general supervised problems that they always have a ground truth for every output.

To solve this problem, we propose the self-supervised method. We use the paired data $y \in \{x, y\}$ as a fake reference of the input image x , then the required mapping can be rewritten as $G : (\mathcal{X}|\mathcal{Y}) \rightarrow \mathcal{Y}^y$, and the desired output should be the same as the image y . However, this leads to another problem that y has much more semantic similarities with x than other random references, and in the test time, the auxiliary image $\mathcal{W}(x, r)$ would be much worse than the self-mapping result $\mathcal{W}(x, y)$ in terms of image quality as well as match accuracy. Inspired by [24], we post-process the auxiliary image $\mathcal{W}(x, y)$, shown in Fig.4. The post-processing includes patches shifting, patterns repeating, and random matches with a certain possibility, to simulate the mismatches and inaccuracy in $\mathcal{W}(x, r)$. Hence the network can learn to fix the inconsistency between $\mathcal{W}(x, r)$ and the output in terms of locations, color, and shape.

This also explains that why we separate the semantic match module from the training network, it would be too easy for the network to generate auxiliary images if it is an end-to-end fashion. Since by using the self-supervised method, the input and the reference are paired data with corresponding features, and the network only need to learn to copy the ground truth

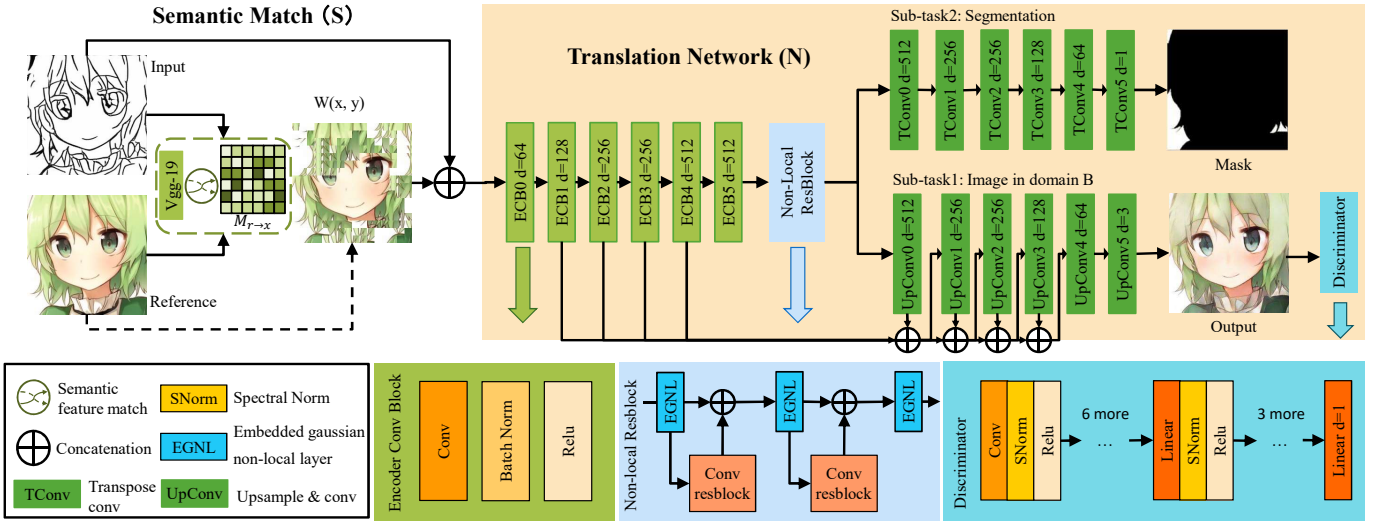


Fig. 2: In the SEGIN model shown at the left is the semantic-match block, mechanism of which is stated in later sub-sections, $\mathcal{W}(x, y)$ obtained by semantic-match is then fed into the major network (shown on the right side) together with the input and the reference. There are two sub-tasks included in the translation network \mathcal{N} , namely generating the images in target domains and the attention segmentation masks. Embedded Gaussian non-local layers are used in the middle Resblock while Spectral normalization layers [21] are adopted in the discriminator.

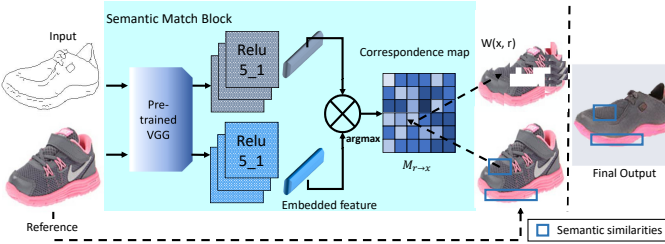


Fig. 3: Semantic match: Image features are first extracted from the input and the reference respectively, cosine distance between the feature points are then calculated and it generates the correspondence map $M_{r \to x}$. Reference image patches can be matched to the input based on the map, and those semantic and spatial information can finally be preserved in the output.

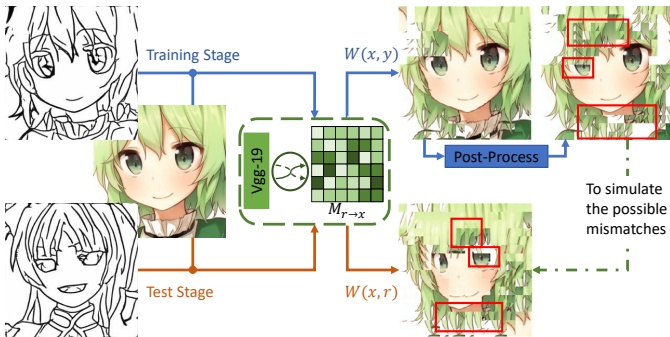


Fig. 4: Data construction and post-process

and make it as the auxiliary image $W(x, y)$. However, such the method cannot generate valid auxiliary image $W(x, r)$ in the test stage when the reference has obvious structural difference from the input. With a separated process for generating the

auxiliary images, followed by a post-processing, the semantic match can be functional in both training and test time.

2) **Architecture:** We use an auto-encoder structure for the generator G of the translation network \mathcal{N} , which contains one encoder and two decoders for separated sub-tasks. The "U" net design [25] is adopted in our major decoder namely the decoder for generating images in the target domain. To improve the propagation of local features, we apply a non-local block at the bottle neck layer of the generator. In our model, we use one discriminator for the major task, where and spectral normalization [21] is applied. In the initial experiment, we found that it was hard to output objects with smooth and complete surfaces, especially for the cases that foreground data distribution is very different than the background. Inspired by TextureGAN [29], which used the segmentation directly as the input, we found that the segmentation can provide information similar to the attention mask mentioned in [20]. With that information, the network can focus on approximating the data distribution within the segmentation mask. However, it is not easy for users to obtain the segmentation masks in a real application if it is required as an input. Therefore, in our major network \mathcal{N} , we use the multi-task structure that the major task (sub-task 1) is to generate images in the target domain, while the auxiliary task (sub-task 2) aims to generate a segmentation distinguishing the foreground from the background of the ground truth images. It can therefore encourage the model to learn information about the attention area.

Moreover, there are cases that $\mathcal{W}(x, r)$ only contains a few valid pixels in a small region. Due to the limited receptive field used in the convolutional neural network, information cannot be propagated to a relatively large region. This issue is more serious when reliable guidance in $\mathcal{W}(x, r)$ are sparse, and the output image tends to be black or grayish since few data is generated based on the reference r . To solve this problem, we

adopt the non-local method [28] by adding non-local layers into our translation network N . The general non-local operation is defined as:

$$\mathbf{y}_i = \frac{1}{\mathcal{C}(x)} \sum_{\forall j} \mathcal{F}(\mathbf{x}_i, \mathbf{x}_j) g(\mathbf{x}_j) \quad (3)$$

where i is the index of an output position whose response will be computed while j is the index that enumerates all the possible positions. \mathcal{F} is a pairwise function computing affinity between i and all j , and g is a unary function that computes a representation of the input signal at location j . In practice, the non-local blocks can be implemented in various formats by choosing different instantiations for \mathcal{F} . It is also mentioned in [28] that the non-local models are not sensitive to the selection of specific functions, therefore in our model we use the embedded Gaussian function as \mathcal{F} shown in Eq.4.

$$\mathcal{F}(\mathbf{x}_i, \mathbf{x}_j) = e^{\theta(\mathbf{x}_i)^T \Phi(\mathbf{x}_j)} \quad (4)$$

The non-local layer can also provide hints for the misled regions, as long as two regions i, j possess similar content features, style of the region with reliable guidance can also be propagated to the mismatched region, related ablation study are shown in Experiment.

3) **Losses**: The multi-task network is governed by the following objectives.

Self-reconstruction Loss The target of this image generation task, as mentioned before, is a self-supervised process whose output is encouraged to be as similar as possible to the reference which is the ground truth in training stage.

$$\mathcal{L}_{recon}(N) = \mathbb{E}_{x,y,\mathcal{W}}[||y - N(x, \mathcal{W}(x, y))||_1] \quad (5)$$

Feature reconstruction Loss In addition to the self-reconstruction loss, we also add feature reconstruction loss. We extract image feature layers (*relu3_2*) from VGG-19[27] to ensure the high-level similarities between the two images. It is shown in our experiments that feature reconstruction loss can help to accelerate the image formation at the initial stage.

$$\mathcal{L}_F(N) = \mathbb{E}_{x,y,\mathcal{W}}[||\Phi(N(x, \mathcal{W}(x, y))) - \Phi(y)||_1] \quad (6)$$

where $\Phi(\cdot)$ indicates the feature extraction.

Adversarial Loss We employ an adversarial loss to encourage the results of N to be like the real samples from domain \mathcal{Y} . The loss is defined as:

$$\mathcal{L}_{GAN}(N, D) = \mathbb{E}_{x,y,\mathcal{W}}[\log D(x, y)] + \mathbb{E}_{x,\mathcal{W}}[\log(1 - D(N(x, \mathcal{W}(x, y))))] \quad (7)$$

where the discriminator D tries to discriminate between the real samples from domain \mathcal{Y} and the generated samples $N(x, \mathcal{W}(x, y))$. Different from non-GAN based methods [14], [4], our network can learn the distribution of a large dataset and therefore is capable to deal with improper matches in $W(x, r)$. It makes the proposed method robust to generate reasonable results even with auxiliary images containing unreliable guidance.

Total Variation Loss To make the output \hat{y} more smooth and consistent, we also add a total variation loss as an objective.

$$\mathcal{L}_{tv}(\hat{y}) = \sum_{i,j} \sqrt{|\hat{y}_{i+1,j} - \hat{y}_{i,j}|^2 + |\hat{y}_{i,j+1} - \hat{y}_{i,j}|^2} \quad (8)$$

The second sub-task is to predict the segmentation map of the output image, serving as the attention mask. The attention loss is consist of two parts. First, we qualify the segmentation by adding an L1 norm regularization, shown in Eq.9

$$\mathcal{L}_{seg}(N_s) = \mathbb{E}_x[||N_s(x) - y_{seg}||_1] \quad (9)$$

where y_{seg} denotes the segmentation ground truth.

We also want to add more shared information between the two tasks, therefore, we propose segmentation based attention loss which is shown in Eq.10.

$$\mathcal{L}_{segAtt}(N, N_s) = \mathbb{E}_{x,y,\mathcal{W}}[||N_s(x) \otimes N(x, \mathcal{W}(x, y)) - y_{seg} \otimes y||_1] \quad (10)$$

where \otimes represents pixel-wise product. We use the output segmentation as an attention mask, and conduct element-wise product between the mask and the generated image, which is then qualified by an element-wise product of the real segmentation mask and the ground truth image.

The full objective is shown in Eq.11

$$\mathcal{L}_{total} = w_1 \mathcal{L}_{recon} + w_2 \mathcal{L}_F + w_3 \mathcal{L}_{GAN} + w_4 \mathcal{L}_{seg} + w_5 \mathcal{L}_{segAtt} + w_6 \mathcal{L}_{tv} \quad (11)$$

w_i are weights for each objective, obtained according to the most optimal results across all the datasets tested in our work. Experiments on multiple datasets show that image qualities of the outputs of these two tasks can be promoted by each other and enhanced mutually.

IV. EXPERIMENTS

Baseline We evaluate several prior I2I models including pix2pix[11], BiCycleGAN[38], MUNIT[10] as the baseline. Specifically, it is stated in MUNIT[10] that a single image can be used as a style reference in image generation. We also set it as the baseline of image-guided I2I model and conduct related experiments for comparison. Besides, we also compared our results with those non-GAN based work, DIA[14], PNN[4] are typical baseline standing for traditional iteration based image synthesis and parametric image synthesis without GAN. We first compare our results directly with that of those methods. Since those methods have similarities to the semantic match part designed in our framework, we also conduct ablation study that replace our semantic match parts with DIA[14] and PNN[4] to show that it is also possible to use different match methods introducing the semantic guidance, and our architecture is robust and of high flexibility with different auxiliary images.

Dataset We test our method on several typical I2I translation datasets, including edges2photots[32], [36], danbooru2018[2] and face colorization on CelebA[17]. For danbooru[2], we combine the Hed[30] with sketch simplification[26] method to extract the sketch of images, those sketches are then used as training and test data in domain A. This sketch generation



Fig. 5: Results generated by SEGIN (our model) are various and natural. The results show semantic similarities to the given reference. Accordingly, Results 1-6 show that general styles of the reference can be inherited independently in specific locations; Specifically, Result 3 (leather shoe) demonstrates that materials can also be transferred to the outputs.



Fig. 6: Compared to pix2pix and the BiCycleGAN, our model can generate images not only with diversity but also controlled by reference; We also compare our model with MU:NIT in terms of similarity to the reference, we use the same references Ref_i for both MUNIT and our models, and we observe that (1) Our results are of higher semantic similarity to the reference (e.g. in the 2nd row, MUNIT failed to generate high heel shoes with blue or brown lining); (2) With similar reference, modal collapse happens in the MUNIT model.(MUNIT 1 and MUNIT 2 in the last row)

method can provide better sketch compared to the original sketches obtained by HED[30] used in edges2photos dataset, some results based on such improved sketches are shown in Appendix. As for the segmentation used in the training stages, we simply pick colored regions as foreground and the remaining parts as background for danbooru2018[2] and CelebA[17]. The segmentation of edges2photos can be found in the work TextureGAN[29]. All the models are trained with 256x256 images;

General settings Our major network contains an encoder for the reference and the input image, two decoders for the target image and the segmentation. We use 6 combined convolution blocks with Relu activation layer and batch normalization layers for the encoder and add 3 non-local layers in total at the bottleneck. Residual blocks with two 3x3 convolutional blocks are used in between non-local layers. To avoid checkerboard effects mentioned in the previous work[22], we use a combination of

up-sample and convolution to replace deconvolution layers in the decoders of sub-task1. Instead of using batch normalization, we adopt spectral normalization[21] as training stabilization techniques in our discriminator to achieve better image quality. We adopted different learning rate for the generator ($2e^{-4}$) and discriminator ($1.3e^{-5}$), and for weights of different objectives are: $w_1 = w_4 = 100.0, w_2 = 5e^{-6}, w_4 = 1.0, w_5 = w_6 = 10.0$, parameters are kept as the same for all the experiments in this work unless specific modification is mentioned later. For datasets containing more than 50K images(sketch2shoes[32], sketch2bags[36], celebA[17]), we use a batch size of 5 and around 20 epochs to achieve satisfactory and stable results. With two NVIDIA 2080Ti GPUs, it takes about 20 hours to finish the training. For smaller datasets, 12-epoch with training time around 10 hours should be enough. For all the datasets, the test time required by the translation network is around 0.03s while the semantic match cost about 1s for a single image.



Fig. 7: We test our model on danbooru[2] anime dataset for sketch \rightarrow anime task. It can be observed that many semantic characteristics of the reference including eyes, hairs, blush, etc. are preserved in the generated results.

A. Qualitative Evaluation

We qualitatively compare our model SEGIN with the previously mentioned models, and the comparison results on the edge2shoes dataset are shown in Fig.6. It can be observed that pix2pix can only output a deterministic result for an input, BiCycleGAN can output results with diversity, but styles of the output cannot be controlled specifically. MUNIT adds image references to guide the output but obtains relatively blurry results with artifacts. Moreover, outputs of the MUNIT can only preserve the style of the reference at an overall level. We notice that SEGIN presents similarities to the reference semantically, it can also maintain semantic details of the reference including different color distribution at specific locations and object materials(i.e. leathers, canvas, suede surface, etc.). More results on the aforementioned dataset are shown in Appendix.

Examples in different datasets are shown in Fig.7-8, we observe that SEGIN are of diversity, realistic as well as semantic similarities to the corresponding reference. In the anime dataset, SEGIN generates images with similar eyes, hairs as well as blushers to that of the reference. Furthermore, in the CelebA dataset, we observe that not only skin color but also the makeup on the reference can be transferred to the outputs. We add the comparison between our work and the non-GAN based methods (i.e., DIA[14], PNN[4]), results are shown in Fig.9. It is obvious that the results of PNN[4] is quite blurry, especially at the image boundaries. While the results of DIA[14] shows that results may be unreasonable when it cannot find the correct corresponding patches in the reference. That is, those methods purely relying on matching output invalid (DIA[14]) or blurry (unnatural) results (PNN[4]) when the correspondences are unreliable. In contrast, our GAN-based framework shows higher robustness, since it can learn to repair mismatched regions from a large dataset within a specific distribution.

B. Quantitative Evaluation

We perform a quantitative evaluation on the edges2photos dataset for the baseline models and SEGIN to analyze the

generated results in terms of diversity, reconstruction capability, and similarities to the reference.

Realistic To evaluate the authentic of our generated results. We use the Fréchet Inception Distance FID score [9] to measure the distribution similarity between our results and the ground truth dataset, results are shown in Table. It can be observed that results generated by SEGIN achieve the best score. I.

Diversity We use LPIPS metric[34] (AlexNet[12] based) to measure the translation diversity, similar to [38], we compute the average LPIPS distance between pairs of randomly-sampled translation output from the same input. 19 pairs sampled outputs with different reference from 100 inputs are tested in both edge2shoes and edge2handbag dataset. The LPIPS scores are shown in Table I, we observe that with various reference, SEGIN achieves the highest score in the experiments. Pix2pix with noise can only produce outputs with a slight variance while BiCycleGAN and MUNIT can achieve similar scores and present relatively lower diversity compared to SEGIN.

We also found that modal collapse happened in prior models given reference images with similar styles shown in the 4th column(MUNIT 1 and MUNIT 2) in Fig.6, to understand this, we analyze the latent space on the MUNIT. Style code \vec{S} is extracted by the encoder in the MUNIT and it seems that this specific modal collapse is caused by the collapse of the style latent space since the vector-like can only store limited information. With similar reference, specifically, the black shoes reference in the 4th column in Fig.6, their extracted style codes are extremely alike. Since our results preserve the spatial information obtained by semantic-match, the final outputs can be of obvious difference. We compute the LPIPS (ref) score for both MUNIT and SEGIN with 20 manually selected similar references for 200 input on the edge2shoes dataset and compare the results guided by the same reference at a time. The style distance of MUNIT and the LPIPS (ref) score of both MUNIT and SEGIN are shown in TableI, it can be observed that SEGIN can remain relatively higher diversity even with similar reference.

Similarity To evaluate the similarity between generated

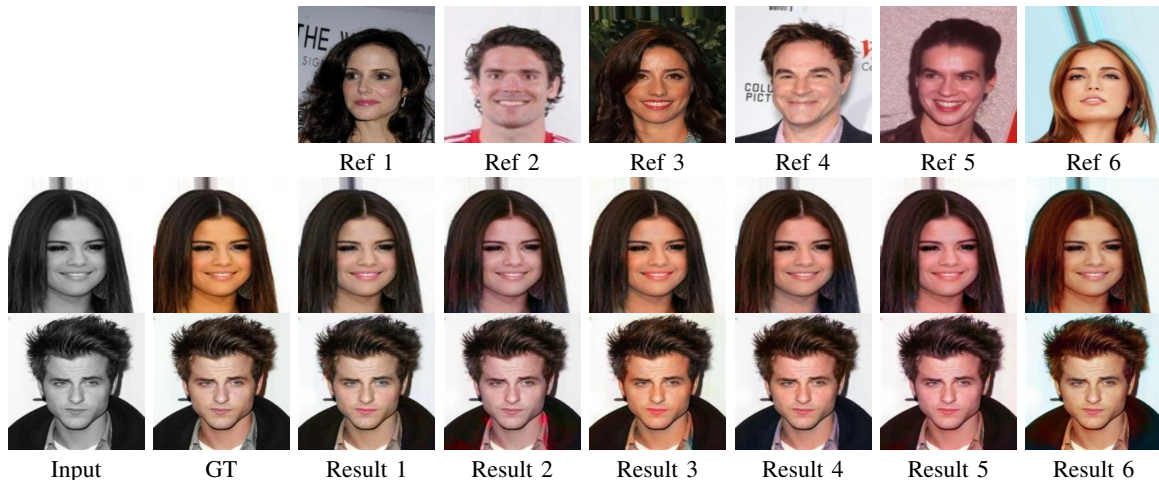


Fig. 8: We also test our model for face colorization on the CelebA[17]. Generated images inherit the style from the reference semantically, only the color of facial elements like skin, lips, etc. are changed accordingly.

Method	edges \rightarrow shoes				edges \rightarrow bags			
	FID	LPIPS	LPIPS (ref)	LPIPS (gt)	FID	LPIPS	LPIPS (ref)	LPIPS (gt)
pix2pix+noise[11]	75.442	0.012	-	0.188	83.241	0.012	-	0.253
BiCycleGAN[38]	62.521	0.108	-	0.152	70.117	0.162	-	0.237
MUNIT[10]	80.857	0.110	-	0.164	88.641	0.171	-	0.239
MUNIT+ref	80.873	0.104	0.467	0.164	89.273	0.158	0.650	0.239
SEGIN (ours)	54.514	0.145	0.382	0.112	68.211	0.211	0.487	0.158
real data	-	0.301	-	0.000	-	0.423	-	0.000

TABLE I: LPIPS distance (the higher the better) indicates the output diversities given input and reference. Paired LPIPS scores (the lower the better) including LPIPS (ref) and LPIPS (gt) that shows the similarity between generated images and the reference and reconstruction capability of models, respectively. SEGIN achieves all the best results, which are also highlighted in this table.

images $G(x, r)$ and the reference r , we compute the average LPIPS (ref) score for pairs of images between the outputs and the reference, 200 image pairs are tested with 10 references on the edge2photos dataset. In this test, we only compare to MUNIT that supports reference guided style control as well. Mostly, the reference may be of difference with the outputs in shape and structure, SEGIN can still achieve a relatively low score (a lower score indicates smaller distance) of 0.382 compared to MUNIT+ref (0.467) in the edge2shoes dataset, and it also outperforms MUNIT model on the edge2handbags dataset with a lower LPIPS (ref) score.

Reconstruction Capability We also evaluate the reconstruction capability for all baseline models and SEGIN as a quantitative way to judge the visual realism of the results. For pix2pix and the BiCycleGAN, we compute the LPIPS[34] scores between the ground truth y and the generated results, where BiCycleGAN generates images with the encoded style data. As for MUNIT and SEGIN, we use the ground truth as a reference to guide the models to generate images as similar as possible to the ground truth, and then we evaluate the LPIPS between paired generated images and the ground truth. In Table I, our model SEGIN outperforms these baselines in terms of the reconstruction quality.

C. Ablation Study

We present an ablation study for the losses used in our model, shown in Fig.11. It can be observed that without the GAN loss, the results are flat and lack of realism though it can maintain most of the features. Output without L_{Recon} and L_F are shown in the 6th and the 7th column respectively, apparent color differences between the generated images and that of the reference can be noticed when not employing reconstruction loss, while severe artifacts can be observed without L_F . Compared to those major loss functions, the TV loss has a relatively slighter impact on the results, but it does help to smooth the images and reduce incoherent variation within one image. Color in the yellow shoes (the first row), changed sharply when not using the TV loss, and the result seems like mottled with white and yellow patches while the result with TV loss is pretty natural and of color consistency. Quantitative results are included in the ablation study as well. We use the Fréchet Inception Distance (FID) [9] to measure the distribution of generated outputs and that of the real images and meanwhile we calculate the LPIPS pair score mentioned previous to assess the reconstruction ability of model without applying certain loss functions, results of which are shown in Table. II.



Fig. 9: Comparison with the non-GAN based image synthesis methods. It can be observed that results of DIA[14] can be invalid if there is no proper corresponding patches between the input and the reference while the results of PNN[4] are quite blurry. GAN can learn to generate images in the target domain even with little hints and corresponding information.

Method	edges \rightarrow shoes		edges \rightarrow bags	
	FID	LPIPS (gt)	FID	LPIPS (gt)
w/o GAN	55.618	0.112	69.981	0.158
w/o L_{recon}	59.162	0.121	78.301	0.174
w/o L_F	76.554	0.147	96.454	0.211
w/o L_{tv}	58.181	0.111	72.538	0.155
w/o NL	72.387	0.132	94.113	0.172
w/o MT	77.211	0.144	98.240	0.181
SEGIN	54.514	0.112	68.211	0.158

TABLE II: FID and LPIPS Pair score of results in the ablation study. SEGIN achieves the best FID scores in both datasets as well as relatively lower LPIPS (gt) score compared to most of other methods. Results without TV loss L_{tv} obtained the lowest LPIPS (gt) score since the smoothness may cause differences during reconstruction. However, with the TV loss, the overall image looks more authentic and achieves much better FID score.

We also conduct ablation experiments to demonstrate that the non-local block and the multi-task framework have an essential contribution to improve the output in terms of color propagation as well as the generation of complete object boundary. We notice that color cannot be propagated properly in the results generated without the non-local layers. While without the multi-task framework that can generate attention mask, the output disposes of artifacts around the edge of objects. We also found those artifacts in prior works[11], [10], and it can be eliminated by generating the attention mask as auxiliary information. We show some ablation study results in Fig.11

It is also possible to use different match methods to replace the semantic match module. Traditional methods to locate the correspondence such as SIFT Flow[15] and results generated

by DIA and PNN can also be considered as the corresponding matching produced in different ways. We perform an ablation study to show that our network has the robustness to output reasonable outputs even with different matching methods while current semantic match generates the best results. Shown in Fig.10, we feed the results of SIFT[15], DIA[14] and PNN[4] into our translation network respectively as auxiliary images. It can be observed that the output images are still of high quality even some of those auxiliary images are invalid or blurry.

V. CONCLUSION

In this paper, we propose a novel I2I translation method that the generated outputs can not only learn a many-to-many mapping between two visual domains but also be guided by reference images semantically. We present a semantic match approach to find corresponding matched patches between two visual contents and model the generator with a multi-task framework as well as non-local layers, which is trained in a self-supervised manner. Both qualitative and quantitative evaluation demonstrates that our method produces realistic and diverse results with higher semantically similarity to the reference compared to the state-of-art prior works. However, there are also limitations in this work: (1)our model requires both input and the reference contains semantic information; (2)when the semantic relation between the input and the reference is weak, the translation will be degraded with only global guidance, the failure case can be found in the Appendix.

REFERENCES

- [1] Amjad Almahairi, Sai Rajeswar, Alessandro Sordani, Philip Bachman, and Aaron Courville. Augmented cyclegan: Learning many-to-many mappings from unpaired data. *arXiv preprint arXiv:1802.10151*, 2018.
- [2] Gwern Branwen Aaron Gokaslan Anonymous, the Danbooru community. Danbooru2018: A large-scale crowdsourced and tagged anime illustration dataset. <https://www.gwern.net/Danbooru2018>, January 2019.
- [3] Aayush Bansal, Yaser Sheikh, and Deva Ramanan. Pixelnn: Example-based image synthesis. *arXiv preprint arXiv:1708.05349*, 2017.
- [4] Aayush Bansal, Yaser Sheikh, and Deva Ramanan. Pixelnn: Example-based image synthesis. *arXiv*, 2017.
- [5] Qifeng Chen and Vladlen Koltun. Photographic image synthesis with cascaded refinement networks. In *Proceedings of the IEEE International Conference on Computer Vision*, pages 1511–1520, 2017.
- [6] Leon A Gatys, Alexander S Ecker, and Matthias Bethge. Image style transfer using convolutional neural networks. In *Proceedings of the IEEE conference on computer vision and pattern recognition*, pages 2414–2423, 2016.
- [7] Arnab Ghosh, Viveka Kulharia, Vinay P Nambodiri, Philip HS Torr, and Puneet K Dokania. Multi-agent diverse generative adversarial networks. In *Proceedings of the IEEE Conference on Computer Vision and Pattern Recognition*, pages 8513–8521, 2018.
- [8] Abel Gonzalez-Garcia, Joost van de Weijer, and Yoshua Bengio. Image-to-image translation for cross-domain disentanglement. In *Advances in Neural Information Processing Systems*, pages 1287–1298, 2018.
- [9] Martin Heusel, Hubert Ramsauer, Thomas Unterthiner, Bernhard Nessler, and Sepp Hochreiter. Gans trained by a two time-scale update rule converge to a local nash equilibrium. In *Advances in Neural Information Processing Systems*, pages 6626–6637, 2017.
- [10] Xun Huang, Ming-Yu Liu, Serge Belongie, and Jan Kautz. Multimodal unsupervised image-to-image translation. In *Proceedings of the European Conference on Computer Vision (ECCV)*, pages 172–189, 2018.
- [11] Phillip Isola, Jun-Yan Zhu, Tinghui Zhou, and Alexei A Efros. Image-to-image translation with conditional adversarial networks. In *Proceedings of the IEEE conference on computer vision and pattern recognition*, pages 1125–1134, 2017.
- [12] Alex Krizhevsky, Ilya Sutskever, and Geoffrey E Hinton. Imagenet classification with deep convolutional neural networks. In *Advances in neural information processing systems*, pages 1097–1105, 2012.



Fig. 10: Ablation study for the matching methods. We adopt the outputs of SIFT[15], DIA[14] and PNN[4] as the matching results and feed them into the translation network \mathcal{N} to demonstrate that \mathcal{N} can generate reasonable results even with other matching methods.



Fig. 11: Ablation study of losses

- [13] Hsin-Ying Lee, Hung-Yu Tseng, Jia-Bin Huang, Maneesh Singh, and Ming-Hsuan Yang. Diverse image-to-image translation via disentangled representations. In *Proceedings of the European Conference on Computer Vision (ECCV)*, pages 35–51, 2018.
- [14] Jing Liao, Yuan Yao, Lu Yuan, Gang Hua, and Sing Bing Kang. Visual attribute transfer through deep image analogy. *arXiv preprint arXiv:1705.01088*, 2017.
- [15] Ce Liu, Jenny Yuen, and Antonio Torralba. Sift flow: Dense correspondence across scenes and its applications. *IEEE transactions on pattern analysis and machine intelligence*, 33(5):978–994, 2010.
- [16] Ming-Yu Liu, Thomas Breuel, and Jan Kautz. Unsupervised image-to-image translation networks. In *Advances in Neural Information Processing Systems*, pages 700–708, 2017.
- [17] Ziwei Liu, Ping Luo, Xiaoang Wang, and Xiaoou Tang. Large-scale celebrities attributes (celeba) dataset.
- [18] Liqian Ma, Xu Jia, Stamatios Georgoulis, Tinne Tuytelaars, and Luc Van Gool. Exemplar guided unsupervised image-to-image translation. *arXiv preprint arXiv:1805.11145*, 2018.
- [19] Michael Mathieu, Camille Couprie, and Yann LeCun. Deep multi-scale video prediction beyond mean square error. *arXiv preprint arXiv:1511.05440*, 2015.
- [20] Youssef Alami Mejjati, Christian Richardt, James Tompkin, Darren Cosker, and Kwang In Kim. Unsupervised attention-guided image-to-image translation. In *Advances in Neural Information Processing Systems*, pages 3693–3703, 2018.
- [21] Takeru Miyato, Toshiki Kataoka, Masanori Koyama, and Yuichi Yoshida. Spectral normalization for generative adversarial networks. *arXiv preprint arXiv:1802.05957*, 2018.
- [22] Augustus Odena, Vincent Dumoulin, and Chris Olah. Deconvolution and checkerboard artifacts. *Distill*, 1(10):e3, 2016.
- [23] Taesung Park, Ming-Yu Liu, Ting-Chun Wang, and Jun-Yan Zhu. Semantic image synthesis with spatially-adaptive normalization. In *Proceedings of the IEEE Conference on Computer Vision and Pattern Recognition*, 2019.
- [24] Xiaojuan Qi, Qifeng Chen, Jiayi Jia, and Vladlen Koltun. Semi-parametric image synthesis. In *Proceedings of the IEEE Conference on Computer Vision and Pattern Recognition*, pages 8808–8816, 2018.
- [25] Olaf Ronneberger, Philipp Fischer, and Thomas Brox. U-net: Convolutional networks for biomedical image segmentation. In *International Conference on Medical image computing and computer-assisted intervention*, pages 234–241. Springer, 2015.
- [26] Edgar Simo-Serra, Satoshi Iizuka, and Hiroshi Ishikawa. Mastering Sketching: Adversarial Augmentation for Structured Prediction. *ACM Transactions on Graphics (TOG)*, 37(1), 2018.
- [27] Karen Simonyan and Andrew Zisserman. Very deep convolutional networks for large-scale image recognition. *arXiv preprint arXiv:1409.1556*, 2014.
- [28] Xiaolong Wang, Ross Girshick, Abhinav Gupta, and Kaiming He. Non-local neural networks. In *Proceedings of the IEEE Conference on Computer Vision and Pattern Recognition*, pages 7794–7803, 2018.
- [29] Wenqi Xian, Patsorn Sangkloy, Varun Agrawal, Amit Raj, Jingwan Lu, Chen Fang, Fisher Yu, and James Hays. Texturegan: Controlling deep image synthesis with texture patches. In *Proceedings of the IEEE Conference on Computer Vision and Pattern Recognition*, pages 8456–8465, 2018.
- [30] Saining Xie and Zhuowen Tu. Holistically-nested edge detection. In *Proceedings of the IEEE international conference on computer vision*, pages 1395–1403, 2015.
- [31] Sheng You, Ning You, and Minxue Pan. PI-REC: progressive image reconstruction network with edge and color domain. *CoRR*, abs/1903.10146, 2019.
- [32] Aron Yu and Kristen Grauman. Fine-grained visual comparisons with local learning. In *Proceedings of the IEEE Conference on Computer Vision and Pattern Recognition*, pages 192–199, 2014.

- [33] Jiahui Yu, Zhe Lin, Jimei Yang, Xiaohui Shen, Xin Lu, and Thomas S Huang. Generative image inpainting with contextual attention. In *Proceedings of the IEEE Conference on Computer Vision and Pattern Recognition*, pages 5505–5514, 2018.
- [34] Richard Zhang, Phillip Isola, Alexei A Efros, Eli Shechtman, and Oliver Wang. The unreasonable effectiveness of deep features as a perceptual metric. In *Proceedings of the IEEE Conference on Computer Vision and Pattern Recognition*, pages 586–595, 2018.
- [35] Richard Zhang, Jun-Yan Zhu, Phillip Isola, Xinyang Geng, Angela S Lin, Tianhe Yu, and Alexei A Efros. Real-time user-guided image colorization with learned deep priors. *arXiv preprint arXiv:1705.02999*, 2017.
- [36] Jun-Yan Zhu, Philipp Krähenbühl, Eli Shechtman, and Alexei A Efros. Generative visual manipulation on the natural image manifold. In *European Conference on Computer Vision*, pages 597–613. Springer, 2016.
- [37] Jun-Yan Zhu, Taesung Park, Phillip Isola, and Alexei A Efros. Unpaired image-to-image translation using cycle-consistent adversarial networks. In *Proceedings of the IEEE international conference on computer vision*, pages 2223–2232, 2017.
- [38] Jun-Yan Zhu, Richard Zhang, Deepak Pathak, Trevor Darrell, Alexei A Efros, Oliver Wang, and Eli Shechtman. Toward multimodal image-to-image translation. In *Advances in Neural Information Processing Systems*, pages 465–476, 2017.



Prof. Kwong Tak Wu Sam joined City University as a lecturer in the Department of Electronic Engineering in 1989. Before joining City University, he worked for Control Data Canada and Bell Northern Research as diagnostic engineer and member of Scientific Staff, respectively. At present, he is the associate editor of the IEEE transactions on Industrial Informatics and IEEE Transactions on Industrial Electronics, Journal of Information Sciences. He is also the Admissions Officer for the graduate programme in the Department. His research interests are evolutionary algorithms, pattern recognition, digital watermarking, video coding and network intrusion systems.



Jialu Huang is a PhD student in the Department of Computer Science, City University of Hong Kong (CityU) since Sep 2018. Prior to that, she was a research developer in ASML. She received the B.Eng. degree from Sun Yat-Sen University and MSc. degrees from King’s College London. Her primary research interests fall in the fields of Image synthesis, Computer Graphics, Evolutionary Algorithm.



Dr. Liao Jing is an Assistant Professor with the Department of Computer Science, City University of Hong Kong (CityU) since Sep 2018. Prior to that, she was a Researcher at Visual Computing Group, Microsoft Research Asia from 2015 to 2018. She received the B.Eng. degree from HuaZhong University of Science and Technology and dual Ph.D. degrees from Zhejiang University and Hong Kong UST. Her primary research interests fall in the fields of Computer Graphics, Computer Vision, Image/Video Processing, Digital Art and Computational Photography.